


RESEARCH ARTICLE

Open Access



A functional role for the cancer disparity-linked genes, *CRYβB2* and *CRYβB2P1*, in the promotion of breast cancer

Maya A. Barrow¹, Megan E. Martin¹, Alisha Coffey², Portia L. Andrews¹, Gieira S. Jones⁴, Denise K. Reaves¹, Joel S. Parker^{2,3}, Melissa A. Troester^{2,4} and Jodie M. Fleming^{1,2*} 

Abstract

Background: In the USA, the breast cancer mortality rate is 41% higher for African-American women than non-Hispanic White women. While numerous gene expression studies have classified biological features that vary by race and may contribute to poorer outcomes, few studies have experimentally tested these associations. *CRYβB2* gene expression has drawn particular interest because of its association with overall survival and African-American ethnicity in multiple cancers. Several reports indicate that overexpression of the *CRYβB2* pseudogene, *CRYβB2P1*, and not *CRYβB2* is linked with race and poor outcome. It remains unclear whether either or both genes are linked to breast cancer outcomes. This study investigates *CRYβB2* and *CRYβB2P1* expression in human breast cancers and breast cancer cell line models, with the goal of elucidating the mechanistic contribution of *CRYβB2* and *CRYβB2P1* to racial disparities.

Methods: Custom scripts for *CRYβB2* or *CRYβB2P1* were generated and used to identify reads that uniquely aligned to either gene. Gene expression according to race and tumor subtype were assessed using all available TCGA breast cancer RNA sequencing alignment samples ($n = 1221$). In addition, triple-negative breast cancer models engineered to have each gene overexpressed or knocked out were developed and evaluated by in vitro, biochemical, and in vivo assays to identify biological functions.

Results: We provide evidence that *CRYβB2P1* is expressed at higher levels in breast tumors compared to *CRYβB2*, but only *CRYβB2P1* is significantly increased in African-American tumors relative to White American tumors. We show that independent of *CRYβB2*, *CRYβB2P1* enhances tumorigenesis in vivo via promoting cell proliferation. Our data also reveal that *CRYβB2P1* may function as a non-coding RNA to regulate *CRYβB2* expression. A key observation is that the combined overexpression of both genes was found to suppress cell growth. *CRYβB2* overexpression in triple-negative breast cancers increases invasive cellular behaviors, tumor growth, IL6 production, immune cell chemoattraction, and the expression of metastasis-associated genes. These data underscore that both *CRYβB2* and *CRYβB2P1* promote tumor growth, but their mechanisms for tumor promotion are likely distinct.

Conclusions: Our findings provide novel data emphasizing the need to distinguish and study the biological effects of both *CRYβB2* and *CRYβB2P1* as both genes independently promote tumor progression. Our data demonstrate novel molecular mechanisms of two understudied, disparity-linked molecules.

Keywords: Crystallin beta B2, Crystallin beta B2 pseudogene 1, Breast cancer, Cancer health disparities

* Correspondence: jodie.fleming@nccu.edu

¹Department of Biological and Biomedical Sciences, North Carolina Central University, 1801 Fayetteville Street, Mary Townes Science Complex, Durham, NC 27707, USA

²Lineberger Comprehensive Cancer Center, University of North Carolina at Chapel Hill, Chapel Hill, NC, USA

Full list of author information is available at the end of the article



Background

While breast cancer is the most common cancer among women, a survival gap exists among African-American and Caucasian/White women [1]. This disparity has persisted over the last decade, despite notable improvements in survival for both races. Historically, White women of all ages exhibited higher incidence; however, recent data suggest that overall incidence rates have converged [1, 2]. Socioeconomic and other factors, including timely access to care, the quality of care, diet and exercise, as well as environmental, and biological factors have been cited as potential explanations of the survival disparity [3, 4]. For example, a higher prevalence of Basal-like breast cancers, a subtype associated with poorer prognosis, is often touted as a prime contributor to the higher mortality rates in young African-American women [5, 6]. However, recent studies stress that African-American women also have higher mortality within luminal A breast cancers and a higher risk of recurrence scores among estrogen receptor-positive and HER2-negative breast cancers [7–9]. To this point, there have been numerous gene expression studies that have classified biological features that vary by race. These inherent biological differences within the tumors may attribute to poorer outcomes witnessed among African-Americans, though few of these observational studies have experimentally tested these associations [4, 7, 10–13]. Accordingly, these reports underscore the need for more basic mechanistic studies to test the contribution of these biological factors to disease progression and patient outcome.

Crystallin β B2 (CRY β B2) has recently drawn particular interest because of its genetic association with overall survival and African-American ethnicity in multiple cancers, including breast, colorectal, renal cell carcinoma, glioblastoma, and prostate tumors [7, 11, 12, 14–17]. In a small prediction analysis study, 91% of all African-American/Black patients ($n = 33$) and 94% of all White patients ($n = 36$) were correctly classified according to race using CRY β B2 as one of the two-gene signatures in prostate tumors, *PSPHL* being the other gene classifier [12]. Similar prediction analyses have been performed using colorectal and breast tumors [7, 11, 14, 15, 18]. Additional studies have also revealed CRY β B2 to be differentially expressed in non-malignant African-American breast tissue [7, 14]. Thus, this gene has successfully been used as a classifier to distinguish between racial groups. Further, higher CRY β B2 expression has been correlated to poorer outcome in cancer, regardless of race [7, 11, 12, 14–16]. Even with these findings, no study has demonstrated a functional role for CRY β B2 in cancers.

The CRY β B2 protein is an abundant ocular lens protein, and mutations have been associated with congenital cataracts and macular degeneration [19, 20]. Mouse

model studies have also demonstrated *Crybb2*^{-/-} mice have reduced fertility compared with wild-type mice via reduced expression of cell cycle and survival genes [21, 22]. Critical to this study, previous reports have indicated that the CRY β B2 pseudogene, *CRY β B2P1*, and not the parental gene was linked with the observed poor outcome in African-American breast cancers and congenital cataracts in particular ethnicities/populations [23–27]. Pseudogenes are copies of protein-coding genes that no longer produce the same functional product as their parental gene, but still share a high-sequence similarity, and can thus regulate or mediate the function of their parental genes through mechanisms such as the generation of non-coding RNAs (ncRNA). An emergent body of literature clearly shows that pseudogenes perform vital roles in regulating normal tissue growth and the development of some diseases, especially cancers [28]. A critical evaluation of published reports identified that the majority of gene expression microarrays examined indiscriminately detect both CRY β B2 and *CRY β B2P1*, due to their high sequence similarity. Therefore, the potential exists that *CRY β B2P1* expression has confounded prior results. It remains unclear whether either gene, or both genes, is linked to breast cancer outcomes. This study investigates racial expression differences and regulatory relationship between CRY β B2 and *CRY β B2P1*.

Methods

Dataset and data processing: re-quantification of CRY β B2 and *CRY β B2P1*

All available Cancer Genome Atlas (TCGA) breast cancer RNA sequencing alignment files ($n = 1221$) were retrieved from GDC Data Portal (<https://portal.gdc.cancer.gov>). Sequence data aligned to chromosome 22: 25,216,000–25,525,000, which span the CRY β B2 and *CRY β B2P1* genes were extracted for further study. Custom scripts were used to search through the alignment files and identify reads that aligned to either CRY β B2 or *CRY β B2P1*, or both genes. The genomic coordinates for each position of each read were marked as either uniquely-mapped to either gene, or as part of a multi-mapped region. Unique and multi-mapped positions from each alignment file were combined, and those that were consistently unique across all samples were merged to form composite regions of unambiguous alignments. The algorithm was tested and validated by adding synthetic reads that mapped to unique regions for each gene and in the multi-mapped regions to several alignment files. Only after validating each stage of the process was the algorithm applied, and the results were used for downstream analyses.

PySam 0.15.0, a python wrapper for Samtools, was used to quantify the reads that mapped to any of the composite unique regions in either CRY β B2 or *CRY β B2P1*. Since the RNA sequencing reads were 50 nucleotides long, only

unique regions that were greater than 50 nucleotides in length were used to quantify the reads. Reads that were flagged in the alignment files as unmapped, having failed quality checks, secondary reads, or PCR duplicates were excluded. Re-quantified counts for each gene were combined with un-normalized counts for all genes in TCGA breast cancer RNA sequencing, and upper quartile normalized. Normalized counts were $\log_2(x + 1)$ transformed and used for analysis unless specified otherwise.

Cell lines, generation of expression models, cell proliferation, and chemoattraction assays

The SUM159 cell line was obtained from Asterand (Detroit, MI) and all remaining cell lines from American Type Culture Collection (Manassas, VA, Additional file 1: Table S1) with the provided authentication documents, cultured as directed by manufacturers. Cells were authenticated every 6 months via short tandem repeat (STR) profiling. Overexpression lentiviral particles and CRISPR expression vectors were obtained from Genecopoeia (Rockville, MD) and cell transduced or transfected according to the manufacturer's instructions. Transfection was conducted using the Fugene HD reagent (Promega) as directed. Clonal cell lines were established via flow cytometry and antibiotic selection. Proliferation assays were conducted as previously described. Briefly, cells were plated in triplicate for each time point, and at the predetermined concentration for each cell line [29]. Cell counts were taken every 24 h for a total of 96 h using a TC20™ automated cell counter (Bio-Rad, Hercules, CA). Cell chemoattraction assays: Costar Transwell permeable support 3.0- μ m polycarbonate membranes were used according to the manufacturer's protocol. The indicated cell model was plated and grown to 80% confluence on 24-well dishes, washed, then placed in serum-free media for 24 h to condition the media. U937 (ATCC) cells were washed, resuspended in serum-free medium, and plated in the top chamber of Transwell inserts (1×10^5 cells per insert; each model plated in duplicate). Cells migrated through the membrane for 4 h towards the indicated cell model in 24-h conditioned media. After this time, non-migratory cells were wiped from the top surface of the membrane; migratory cells were then fixed in methanol and stained with 1.0% crystal violet. Cell numbers were determined from microphotographs taken over five (non-overlapping) areas of the membrane.

Western immunoblotting and immunocytofluorescence

Cells were lysed in mPer Lysis Buffer (Thermo Scientific, Rockford, IL) supplemented with protease and phosphatase inhibitors (Halt™ Thermo Scientific), then subjected to western analyses as previously described [29–31]. Antibodies: CRYBB2, Novus Biologicals (Centennial, CO; catalogue numbers 001415-M02 and NBP2-13876) and

STAT3, Phospho-Stat3⁷⁰⁵, Actin, Cell Signaling Technology (Danvers, MA; catalogue numbers 9131, 9145, and 4968, respectively). Immunofluorescence was performed with appropriate controls as previously described [32].

Quantitative real-time PCR, subcellular RNA fractionation, and detection of metastatic cells

Total RNA was isolated using the RNeasy kit (Qiagen; Hilden, Germany). Subcellular RNA fractionation was performed using the Active Motif kit #25501 (Carlsbad, CA) following the manufacturer's instructions with the modification of lysis shortened to 2 min. RNA was reverse transcribed using the High Capacity cDNA RT Kit (Life Technologies), and qPCR analysis conducted using the Absolute Blue qPCR Mix, Low Rox (ThermoFisher) with the Applied Biosystems QuantStudio™ 6 Flex Real-Time PCR system each according to the manufacturer's instructions. Relative fold changes in gene expression were determined via the $\Delta\Delta$ CT method and/or the standard curve analysis when indicated. Primer sequences are listed in Additional file 2: Table S2.

Xenograft generation

Animal experiments were conducted in accordance with accepted standards of humane animal care and approved by the Animal Care and Use Committee at North Carolina Central University. Xenografts were generated as we previously described [33]. Briefly, 5-week-old female Hsd: Athymic Nude-*Foxn1*^{tmu} mice (Envigo, Dublin, VA) were injected orthotopically into the right abdominal mammary gland with 5×10^5 of the indicated cell model suspended in 30.0 μ l of 50/50 PBS:Matrigel. Weekly tumor growth was measured via calipers and tumors excised when volume neared 400 mm³. Whole tumors were homogenized and RNA extracted using the Qiagen RNeasy kit as instructed. Three independent experiments were performed to ensure repeatability. Mice that did not form tumors were euthanized 5 months post-injection. Detection of metastatic xenograft cells in liver and lung was conducted as previously described [33].

Three-dimensional morphogenesis assays and live cell imaging

3D cultures were performed as previously described [34–36]. Briefly, equal numbers of proliferating cells were plated on laminin-rich basement membrane gels (growth factor-reduced Matrigel®, Sigma) in culture medium containing 2.0% basement membrane to support 3D growth; 3D growth medium was replaced every 3 days. Cells were imaged on the 10th day of culture, and cell morphology, size/area, organization, and growth were evaluated using a Nikon DiaPhot microscope with digital camera and NIS-Elements 4.11.00 (Nikon Instruments Inc., NY). Live cell imaging was conducted using an InCuCyte®

S3 Live Cell Analysis System (Sartorius) using phase contract, $\times 10$ magnification, one image captured every 4 h for 3 days. Cells were extracted from gels for RNA isolation using the Corning Cell Recovery Solution as instructed.

IL6 signaling inhibition and IL6 ELISAs

IL6 signaling was inhibited using a 24-h dose of 75.0 ng/ml in vitro and 100.0 $\mu\text{g}/\text{kg}$ in vivo intratumoral injection of a recombinant human IL6 receptor blocking antibody or isotype control (R&D Systems, catalogue MAB227 and MAB002) [37]. Inhibition of IL6 signaling was confirmed via STAT3 phosphorylation. ELISA: Proliferating cells were washed and cultured in serum-free media for 24 h. Conditioned medium was collected, centrifuged to remove residual cells, and concentrated via Millipore Amicon™ Ultra-15 Centrifugal Filter Units. Medium was normalized for total protein content and quantitated for total IL6 using the RayBio® Human IL6 ELISA Kit as instructed.

Additional statistical analysis

For all assays, a minimum of three independent experiments were performed using a minimum of duplicate samples in each experiment. For correlation determination, the Spearman correlation was used. Significance was determined via one-way analysis of variance (ANOVA) with Tukey Honest Significant Difference (HDS) or Bonferroni post hoc analyses. *T* tests were also performed using GraphPad Prism Software 6.0 unless otherwise noted. Data was considered significant at $P < 0.05$.

Results

Evaluating *CRYBB2* and *CRYBB2P1* gene expression differences in TCGA breast cancer samples by subtype and race

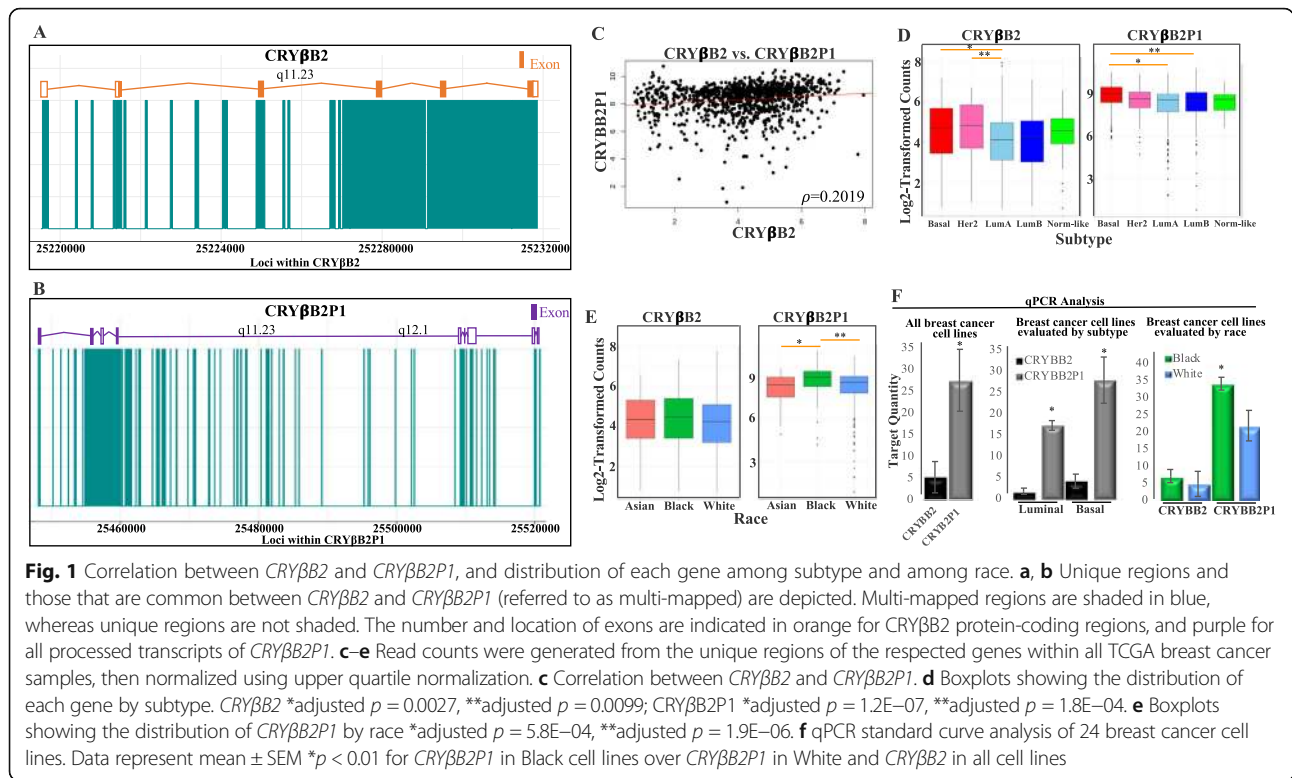
To determine whether there is an independent contribution of *CRYBB2* and *CRYBB2P1* to the promotion of breast cancer and breast cancer disparities, custom scripts were used to search through all available TCGA breast cancer RNA sequencing alignment files ($n = 1221$) to identify reads that aligned to either *CRYBB2* or *CRYBB2P1*, or both genes. The genomic coordinates for each position of each read were marked either as uniquely mapped to either gene or as part of a multi-mapped region (visualized in Fig. 1a, b). Unique and multi-mapped positions from each alignment file were combined, and those that were consistently unique across all samples were merged to form composite regions of alignments.

Patient demographics and tumor subtypes (Table 1) were assessed for associations with the abundance of unambiguous alignments. Samples were first stratified according to race with Caucasian/White women constituting 77.6%, African-American/Black 16.9%, and Asian 5.5% of the total sample set. The luminal A subtype was the most numerous

in White (52.6%) and Asian (33.9%) tumor samples, while Basal tumors were the most numerous subtypes for Black samples (33.9%) compared to all other subtypes evaluated. Assessment of correlation between the unambiguous expression estimates of *CRYBB2* and *CRYBB2P1* resulted in no significant correlation observed between *CRYBB2* and *CRYBB2P1* among all samples (Fig. 1c, $p = 0.2019$; Spearman Correlation). Overall, there were consistently higher counts for *CRYBB2P1* compared to *CRYBB2* in all breast tumor subtypes and ethnicities evaluated (Fig. 1d, e). *CRYBB2* expression was significantly higher in the basal and Her2 tumors compared to luminal A tumors (adj $p = 0.003$ and 0.009 , respectively; one-way ANOVA with Tukey HSD test), while *CRYBB2P1* expression was significantly higher in the basal tumors compared to luminal A and B tumors (adj $p = 1.2\text{E}-07$ and $1.80\text{E}-04$, respectively; one-way ANOVA with Tukey HSD test). Divergent from previous reports, the levels of *CRYBB2* were not significantly different between Asian, Black, and White tumors. However, *CRYBB2P1* had significantly higher expression in Black tumors compared to Asian and White (Fig. 1e, adj $p = 5.8\text{E}-04$ and adj $p = 1.9\text{E}-06$, respectively; one-way ANOVA with Tukey HSD test). These data correspond with a subset of studies that suggest *CRYBB2P1*, and not *CRYBB2*, is the gene associated with health disparities and poor outcome in breast cancers [23, 24]. When evaluating the data by first conditioning based on either subtype or race, the same patterns of significance persisted for each gene with only one exception; *CRYBB2* expression was no longer significantly higher in Her2 compared to luminal A tumors (Additional file 3: Figure S1A&B). The participant demographic factors of age/menopause status were not significant when observing gene distribution among race or subtype for *CRYBB2* (not shown). However, *CRYBB2P1* was significantly differentially expressed by race as well as by subtype after conditioning for race when evaluating age/menopause status (Additional file 3: Figure S1C-E). Most notably, *CRYBB2P1* was significantly higher in postmenopausal Black tumor samples compared to White postmenopausal and perimenopausal, and Asians under 40 years of age (adj. $p = 0.027$, 0.005 , and 0.033 , respectively; one-way ANOVA with Tukey HSD test). To test if similar patterns of expression were observed in breast cancer cell lines, a panel of 24 luminal and basal breast cancer cell lines were evaluated via qPCR using primers specific to either *CRYBB2* or *CRYBB2P1* (cell lines and race are listed in Additional file 1: Table S1). Results corresponded with the patterns observed in tumor samples, with increased transcript abundance of *CRYBB2P1* in basal and Black cell models compared to *CRYBB2* ($p < 0.01$, Fig. 1f).

Loss of *CRYBB2P1* expression increases *CRYBB2* levels

To study the independent effects of each gene, overexpression of *CRYBB2* and *CRYBB2P1* and CRISPR knockout of



CRYBB2P1 cell models from three triple-negative breast cancer (TNBC) cell lines were established (Fig. 2). Basal levels of *CRYBB2* protein in the parental cell models were below detectable levels via immunoblotting from cell cultures growing in 2D but were readily detectable in the overexpression models (Fig. 2a). The most striking observation in all cell models was that the knockout of *CRYBB2P1* resulted in a significant increase of transcript abundance as well as protein expression of *CRYBB2* ($p < 0.01$, t test; Fig. 2b, c). *CRYBB2* was primarily localized to the cytoplasm and pseudopodial structures in both the *CRYBB2* overexpression and *CRYBB2P1* knockout models. Proliferation assays demonstrated that overexpression of *CRYBB2*

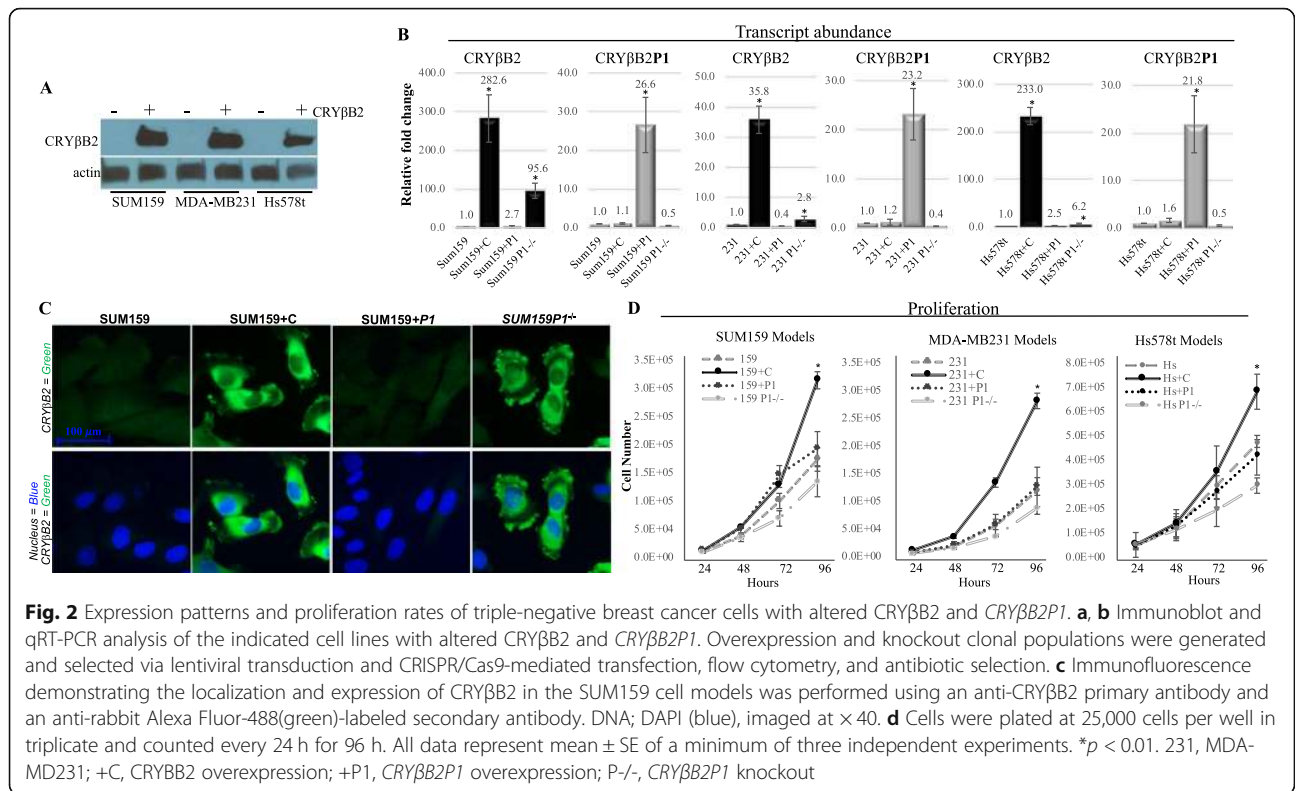
significantly enhanced cell proliferation by subtype compared to the control parental cells as well as *CRYBB2P1* overexpression or knockout models ($p < 0.01$, one-way ANOVA with Bonferroni test; Fig. 2d). Thus, while *CRYBB2P1* knockout increased *CRYBB2* expression, it was not sufficient to produce the enhanced proliferation observed in the *CRYBB2* overexpressing models.

As expression of *CRYBB2P1* repressed expression of *CRYBB2*, CRISPR knockout models of *CRYBB2* and dual overexpression of models of *CRYBB2* and *CRYBB2P1* were generated to obtain a comprehensive analysis of the gene interactions (Fig. 3). *CRYBB2* overexpression and knockout did not alter *CRYBB2P1* transcript abundance.

Table 1 Demographic and tumor characteristics

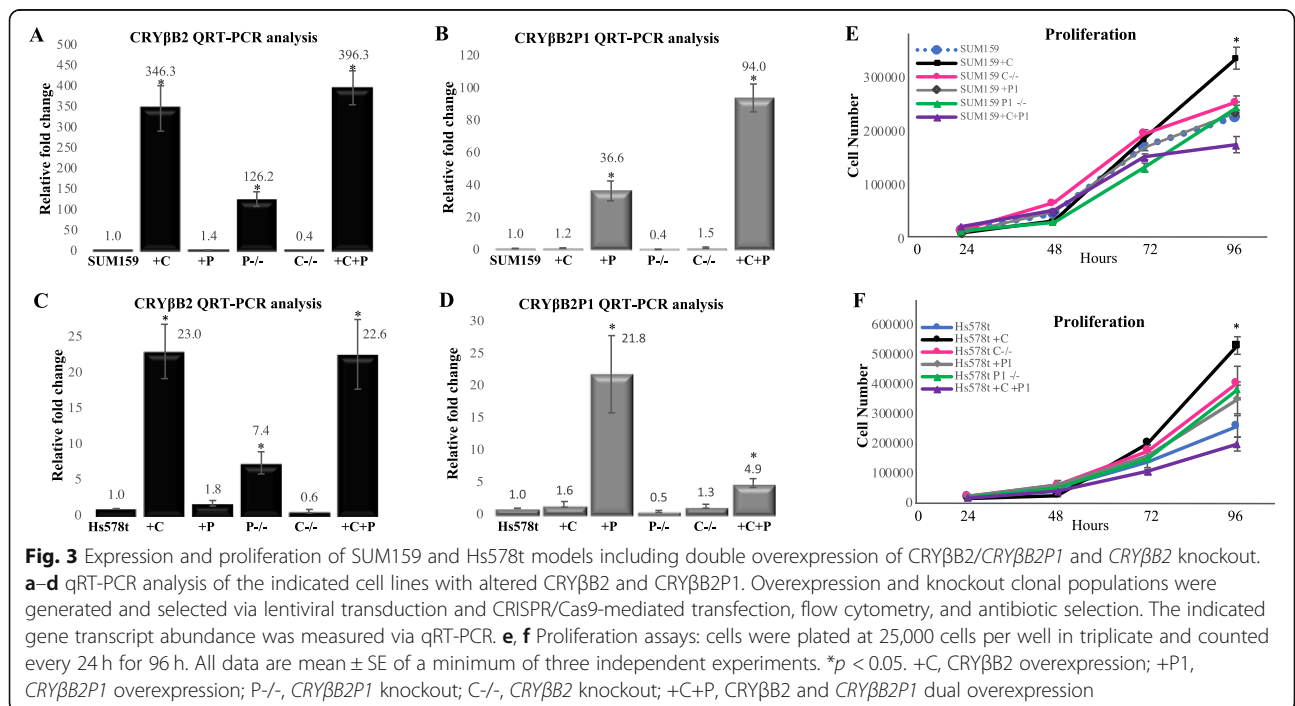
Subtype	Asian (n = 62)	Black (n = 189)	White (n = 867)	Total (N = 1118)
Basal	7 (11.3%)	64 (33.9%)	113 (13.0%)	184 (16.5%)
Her2	16 (25.8%)	16 (8.5%)	39 (4.5%)	71 (6.4%)
Luminal A	21 (33.9%)	62 (32.8%)	456 (52.6%)	539 (48.2%)
Luminal B	16 (25.8%)	31 (16.4%)	137 (15.8%)	184 (16.5%)
Normal like	2 (3.2%)	16 (8.5%)	122 (14.1%)	140 (12.5%)
Race	Young (n = 76)	Pre (n = 111)	Peri (n = 274)	Post (n = 551)
Asian	8 (10.5%)	6 (5.4%)	23 (8.4%)	24 (4.4%)
Black	20 (26.3%)	18 (16.2%)	59 (21.5%)	86 (15.6%)
White	47 (61.8%)	77 (69.4%)	192 (70.1%)	441 (80.0%)

Young, < 40 years; Pre pre-menopausal, 40–46; Peri peri-menopausal, 46–55; Post post-menopausal, > 55 years



These data suggest that while *CRYBB2P1* may function as a non-coding RNA to regulate transcription, *CRYBB2* does not have a significant reciprocal effect on *CRYBB2P1* expression. Cellular fractionation also confirmed that loss of either gene did not alter transcript localization between

the nucleus and cytosolic fractions (Additional file 3: Figure S2). Proliferation assay results show that the dual overexpression of *CRYBB2* and *CRYBB2P1* resulted in the lowest proliferation rates for the Hs578t and SUM159 models tested, and *CRYBB2* overexpression remained the



only genetic alteration capable of significantly altering proliferation in 2D cultures ($p < 0.05$, one-way ANOVA with Bonferroni test; Fig. 3e, f).

CRYBB2 and CRYBB2P1 overexpression independently increase tumorigenicity, and CRYBB2 overexpression enhances detection of metastatic cells within the liver

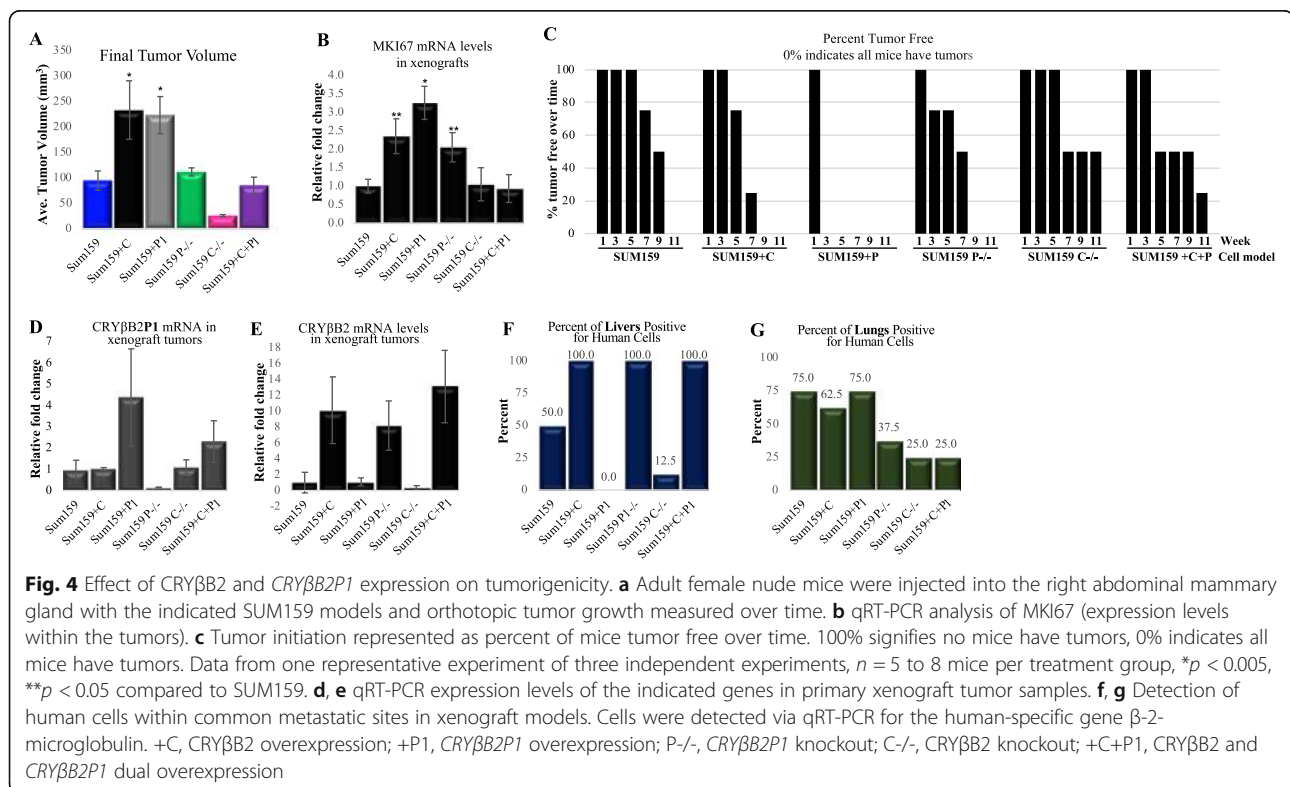
Xenografts using the SUM159 models were used to evaluate tumorigenicity and detection of metastatic cells in common sites of metastasis. Similar to proliferation studies, the CRYBB2-overexpressing cells had significantly larger final tumor volume and increased tumor cell proliferation (indicated by increased *Ki67* expression) compared to parental control cells, gene knockouts, and dual gene overexpression models ($p < 0.005$ and $p < 0.05$, t test; Fig. 4a, b). CRYBB2 knockout had the lowest final tumor volume, and no significant change was observed when comparing the control parental cell line which was observed with the CRYBB2P1 knockout and dual CRYBB2/CRYBB2P1-overexpressing cells. Of note, cells overexpressing CRYBB2P1 alone had significantly larger final tumor volume and significantly increased *Ki67* expression ($p < 0.005$, one-way ANOVA with Bonferroni test). Cells overexpressing CRYBB2P1 also demonstrated increased tumorigenicity, with tumors readily detected in all animals at 3 weeks post-injection compared to other models that exhibited 100% mice bearing tumors after 8 weeks or later (Fig. 4c). Collectively,

these in vivo data suggest additional gene regulatory roles for CRYBB2P1 that are independent of its ability to regulate CRYBB2.

We confirmed that each cell model retained the desired altered gene expression in the primary tumors via qPCR (Fig. 4e, f), then investigated the presence of metastatic human cells in mouse livers and lungs using human-specific Beta-2-Microglobulin primers. Distinct localization patterns were observed for all models overexpressing CRYBB2; 100% of the cells detected in the liver had either CRYBB2 overexpression or CRYBB2P1 knockout, which significantly increases CRYBB2 expression. Loss of CRYBB2 or overexpression of CRYBB2P1 resulted in notably lower levels of detection of cells within the liver (Fig. 4f). This pattern of enhanced detection of cells overexpressing CRYBB2 in the liver was not observed in the lung.

CRYBB2 overexpression alters breast cancer cell growth behaviors in 3D cell culture

To directly observe cellular morphology and behaviors, cultures of all the SUM159 and Hs578t cell models were grown in 3D culture and monitored over 10 days via live cell imaging. Consistent with in vivo study results, the size of spheroids was significantly larger in the models overexpressing CRYBB2, CRYBB2P1, and CRYBB2P1 knockout (which increases CRYBB2 levels) compared to the control parental cell lines ($p < 0.008$, one-way ANOVA



with Bonferroni test; representative images for the SUM159 models shown in Fig. 5 and Additional file 3: Figure S3 for Hs578t models). The increase in sphere size suggests increased proliferation or survival as observed in xenografts. Indeed, increased expression of *Ki67* was detected via qPCR in *CRYBB2P1*-overexpressing, *CRYBB2*-overexpressing, and *CRYBB2P1*-knockout models (which increases *CRYBB2* expression; $p < 0.04$, t test, compared to control parental cell lines, *data not shown*). The most striking observation was the significant increase in invasive structures in cells with high levels of *CRYBB2* (*CRYBB2* overexpression and *CRYBB2P1* knockouts). Total RNA was extracted from 3D cultures grown for 10 days and analyzed via tumor metastasis and epithelial-mesenchymal transition (EMT) pathway-focused qPCR arrays. Table 2 documents the most significant results, highlighting an overall increase in invasive, EMT, and metastatic genes and a suppression of epithelial and metastatic suppressive genes in cells overexpressing *CRYBB2* compared to the control parental SUM159 and Hs578t models.

CRYBB2 overexpression enhances interleukin 6 secretion, signaling, and immune cell attraction

Invasive structures similar to those observed in the *CRYBB2*-overexpressing models were previously observed using 3D cultures of MCF10AI human breast epithelial cells [38]. These invasive structures were shown to be dependent on IL6 stimulation [38]. IL6 was also previously shown to be one of the most significantly increased inflammatory cytokines in African-American breast cancer patients compared to White patients, and

high plasma IL6 levels were identified as a breast cancer risk factor in African-American women [39, 40]. To test if IL6 was contributing to the increased invasive phenotype in *CRYBB2*-overexpressing cells, IL6 production was tested via qPCR and ELISAs in three triple-negative breast cancer model systems. Overexpression of *CRYBB2* significantly induced IL6 expression and secretion in all models tested ($p < 0.01$, t test; Fig. 6a, b). Autocrine/paracrine activation of IL6 signaling was confirmed by evaluating STAT3 activation in four triple-negative breast cancer model systems (Additional file 3: Figure S4). Consistent with the role of IL6 in immune cell chemoattraction, in vitro chemoattraction studies show a trend of increased attraction of monocyte-like U937 cells towards cells overexpressing *CRYBB2* (Fig. 6c, $p = 0.052$, t test).

IL6 also contributes to breast cancer cell proliferation [41]. Correspondingly, inhibition of IL6 signaling using an IL6 receptor blocking antibody demonstrated a decrease in STAT3 activation and the proliferation rate of cells overexpressing *CRYBB2* ($p < 0.01$, t test; Fig. 6d, e). Inhibition of IL6 signaling in the *CRYBB2*-overexpressing cells resulted in no significant difference in growth rates between all *CRYBB2/CRYBB2P1* modified models tested (Fig. 6f). Enhanced IL6 production was correspondingly detected in xenograft tumors with increased levels of *CRYBB2* (Fig. 7a). Xenograft studies were repeated using the IL6R blocking antibody in vivo, and results demonstrate inhibition of IL6 signaling reduced tumorigenesis of SUM159 cells overexpressing *CRYBB2*, but had no significant effect on final tumor volume in *CRYBB2P1*-overexpressing cells (Fig. 7b, c). While tumor proliferation was

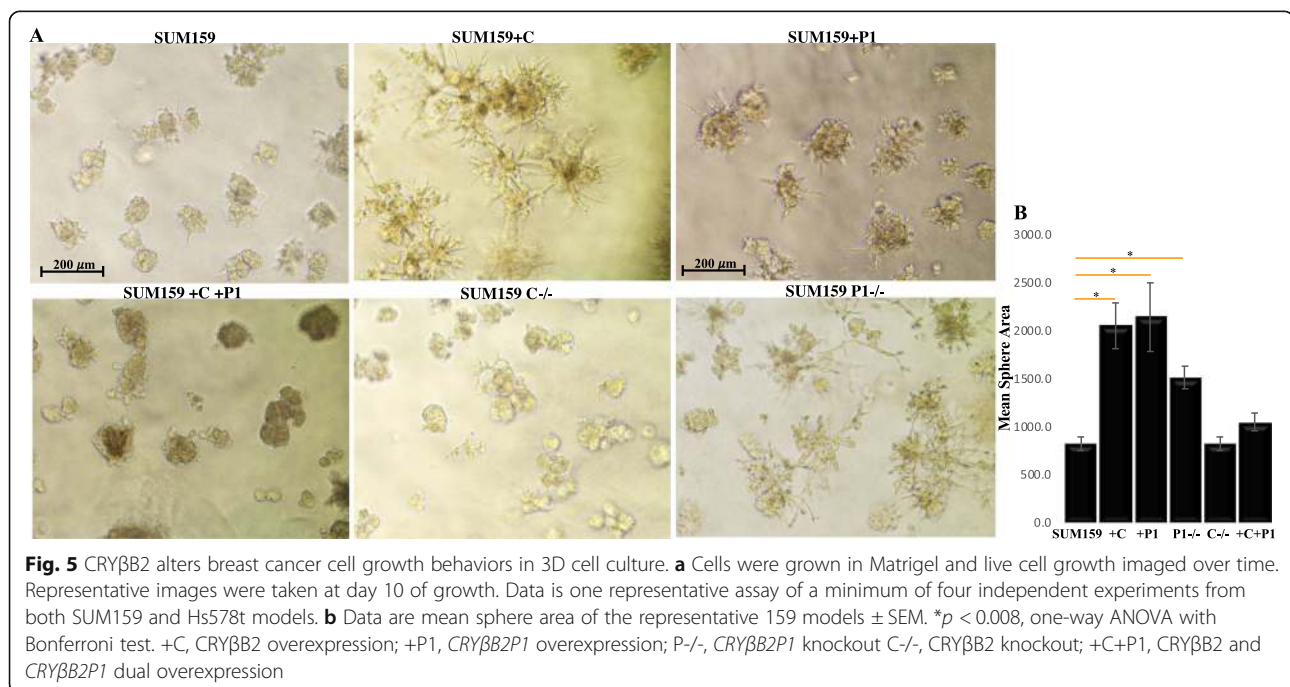


Table 2 Fold change in gene expression of *CRYBB2*-overexpressing cells compared to control cells

Gene symbol	Name	Fold
IL1RN	Interleukin 1 receptor antagonist	15.07
MMP13	Matrix metalloproteinase 13	12.38
IL1B	Interleukin 1 beta	9.45
TSHR	Thyroid-stimulating hormone receptor	5.92
IGF1	Insulin-like growth factor 1	4.93
CDH11	Cadherin 11, type 2, OB-cadherin	4.66
MMP3	Matrix metalloproteinase 3	4.41
FLT4	Fms-related tyrosine kinase 4	3.87
ITGB3	Integrin, beta 3	3.39
MMP9	Matrix metalloproteinase	3.39
VCAN	Versican	3.14
SOX10	Transcription factor SOX-10	2.61
SSTR2	Somatostatin receptor 2	2.53
CTSL	Cystatin F	2.48
RORB	RAR-related orphan receptor B	2.38
TMEM132A	Glucose-regulated protein, 78 kDa	2.14
CDH6	Cadherin 6, type 2, K-cadherin	-10.62
FGFBP1	Fibroblast growth factor binding Prot. 1	-7.78
WNT5B	Wnt family member 5B	-7.32
CDH1	Cadherin 1, type 1, E-cadherin	-6.33
COL3A1	Collagen, type III, alpha 1	-5.63
DSP	Desmoplakin	-5.09
CDKN2A	Cyclin-dependent kinase inhibitor 2A, p16	-4.79
MAP1B	Microtubule-associated protein 1B	-4.22
TGFB2	Transforming growth factor beta 2	-3.88
MST1R	Macrophage-stimulating 1 receptor	-3.14
DSC2	Desmocollin 2	-2.93
WNT11	Wnt family member 11	-2.75
MTSS1	Metastasis suppressor 1	-2.68
KISS1R	KiSS-1 metastasis-suppressor receptor	-2.28
ITGA7	Integrin, alpha 7	-2.2
FGFR4	Fibroblast growth factor receptor 4	-2.18

reduced in xenografts, the invasive phenotype induced by *CRYBB2* overexpression was not decreased when IL6 was inhibited in 3D cultures (Fig. 7d).

Discussion

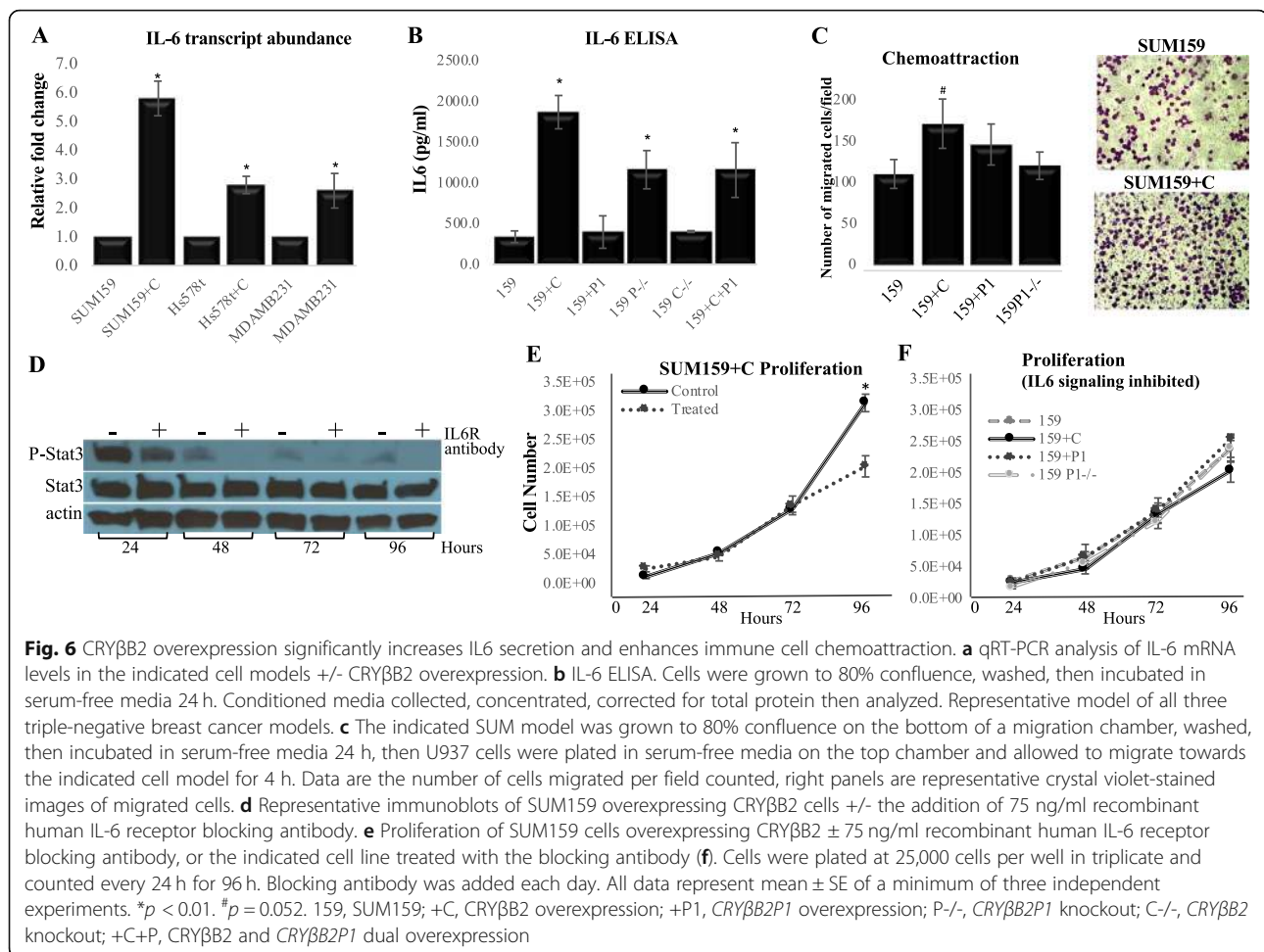
This study demonstrates that both *CRYBB2* and *CRYBB2P1* promote tumor growth, but their mechanisms for tumor promotion are likely distinct. Overexpression of *CRYBB2*, but not *CRYBB2P1*, induces IL6 secretion, cell proliferation in 2D cultures, an invasive phenotype in 3D cultures, and a consistent homing of metastatic cells to the liver. Conversely, *CRYBB2P1* overexpression

promotes tumorigenicity via increasing proliferation, while suppressing *CRYBB2* expression. The suppression of *CRYBB2* by *CRYBB2P1* may be critical for cell function, as our results demonstrate overexpression of both *CRYBB2* and *CRYBB2P1* suppresses cell proliferation and tumor growth. This supports the idea that *CRYBB2P1* may function as an antisense regulator to the parental gene *CRYBB2*.

Previous functional studies have suggested similar results where a gene and its pseudogene have common mechanisms but mutual inhibition. For example, Korneev et al. showed that translation of the neural nitric oxide synthase (NOS) protein was inhibited by expression of the NOS pseudogene [42]. We hypothesize that the suppression of *CRYBB2* expression by the pseudogene may have evolved during gene replication as a protective mechanism to inhibit inappropriate cellular proliferation, but this mechanism has been manipulated by the cancer cell to ensure proliferation and tumor progression. As previously stated, simultaneous overexpression of both *CRYBB2* and *CRYBB2P1* is inhibitory to cell proliferation and tumorigenesis, suggesting a mechanistically distinct, but functional redundancy between the ancestral/parental gene and pseudogene. It is also clear that the mechanism by which *CRYBB2* and *CRYBB2P1* affect tumor promotion vary independently, given the lack of direct correlation/relationship between the expression levels of *CRYBB2* and *CRYBB2P1* in TCGA breast cancer samples. Other studies such as Duret et al. have found evidence that pseudogenes can evolve independently from their parental genes and have independent functions, which may be relevant to the *CRYBB2* and *CRYBB2P1* relationship [43].

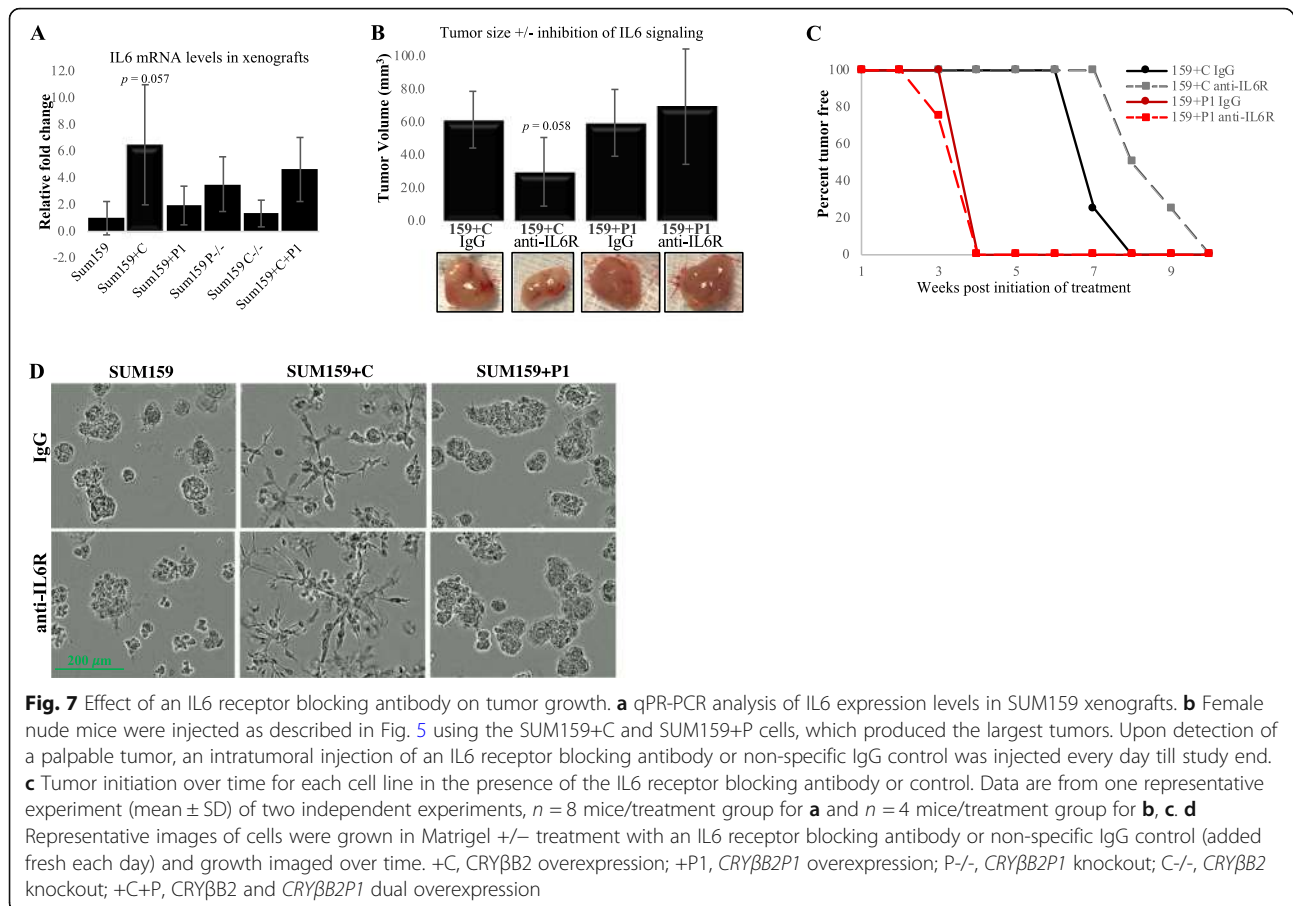
Another major conclusion that can be drawn from our investigation is the distinction of the race-related expression of *CRYBB2* and *CRYBB2P1*. First, our data highlight that expression of the pseudogene, *CRYBB2P1*, is associated with Black/African-American breast cancer patients compared to White and Asian patient samples, and *CRYBB2P1* expression levels are higher compared to *CRYBB2* in all TCGA breast cancer samples. Other studies have highlighted *CRYBB2* as a health disparity gene in breast cancer, but our data suggest technical difficulties in distinguishing between the expression levels of the two genes and that the more likely disparity target is *CRYBB2P1* [7, 11, 12, 14–17]. Second, our data suggest *CRYBB2P1* functions as a ncRNA in triple-negative breast cancers to alter transcription.

Pseudogenes are copies of protein-coding genes that no longer produce the same functional product as their parental gene, but still share a high sequence similarity, and can thus regulate or mediate the function of their parental genes through mechanisms such as the generation of ncRNA. Pseudogenes can be transcribed in parallel with their parental genes, or with their own tissue



or temporal specific patterns [28]. Evidence shows that pseudogenes perform vital roles in regulating normal tissue growth and the development of some diseases, especially cancers [28]. They can serve as antisense regulatory transcripts or miRNA decoy, produce siRNAs or ncRNAs, and encode short proteins [44]. For example, *Lethe* is a pseudogene that produces a ncRNA. The pseudogene ncRNA is selectively induced by pro-inflammatory cytokines via NF κ B and functions in negative feedback signaling to NF κ B [45]. The genomic-wide effect of *CRYBB2P1* is currently under investigation in our laboratory. Of note, a review of seven cancer lines in the publicly available University of California, Santa Cruz, genome browser database indicates *CRYBB2P1* is active (marked with active histone mark, H3K4me3) and rich in transcription factor and chromatin regulatory marks, while not many regulatory marks are present for *CRYBB2*. These data strongly suggest *CRYBB2P1* ncRNA may act in cis at the *CRYBB2* locus and/or function in trans genome-wide.

One limitation of the current study is the focus on triple-negative breast cancers. We have previously reported *CRYBB2* as one of four genes significantly associated with African-American race and survival in luminal A breast cancers [7]. Data presented herein clearly show a role for *CRYBB2* independent of *CRYBB2P1* in the promotion of breast cancer, including increased proliferation, tumorigenesis, and invasive behaviors. Whether *CRYBB2P1* alters *CRYBB2* expression, or has tumor-promoting effects independent of *CRYBB2*, specifically in luminal cells was not investigated. Another constraint of our study is that although triple-negative breast cancer is a heterogeneous disease, we restricted our TCGA and cell line analyses to basal-like subtypes [46–49]. While multiple subtype classification methods for TNBCs currently exist, the basal subtype comprises over 70% of the TNBC subtype. Restricting our analyses to basal-like subtypes reduces experimental heterogeneity and increases generalizability of our results. In addition to cancer subtype specificity, we acknowledge the potential that exists that the influence of *CRYBB2* and



CRYBB2P1 on tumor cell behaviors is tissue dependent. Pilot studies in our laboratory show *CRYBB2* but not *CRYBB2P1* is expressed significantly higher in pancreatic cancer cell lines compared to primary pancreatic cells (Additional file 3: Figure S5).

The data presented herein demonstrate a set of biological functions and physiological consequences of high *CRYBB2* protein expression in breast cancer models. Overexpression of *CRYBB2* increased IL6 production, upregulated the expression of proliferative genes, and increased proliferation of breast cancer cells in vitro and in vivo. *CRYBB2* also induced EMT/metastatic phenotypes in triple-negative breast cancer cells including the upregulation of a set of genes known to increase tumor metastasis in vivo. Sox10 was one gene of note that was significantly upregulated in *CRYBB2*-overexpressing cells. A recent eloquent study by Dravis et al. demonstrated that in both mouse and human tumors, SOX10 expression correlates with stem/progenitor identity, dedifferentiation, and invasive characteristics, and DNA binding motifs for SOX transcription factors are enriched in stem/progenitor cells [50]. This data suggests the potential for the upregulation of SOX10 and IL6 in *CRYBB2*-overexpressing cells mediating the trans-differentiation to an invasive, EMT-like phenotype.

Conclusions

In summary, our findings support a mechanistic role in racial differences for *CRYBB2*, but suggest that *CRYBB2P1* is a relevant disparities target. We provide novel data emphasizing the need to distinguish the biological effects of *CRYBB2* and those of the ncRNA, *CRYBB2P1*, as overexpression of either gene enhances tumor progression. Our studies demonstrate that *CRYBB2P1* can enhance tumorigenesis in vivo, and loss of *CRYBB2P1* expression results in significantly increased *CRYBB2* levels. To our knowledge, we are the first to report physiological consequences of breast cancer cells that have high *CRYBB2* expression including increased tumor proliferation, IL6 secretion, enhanced metastatic homing to the liver, increased expression of metastatic and EMT-associated genes, and invasive cellular behaviors. These data are highly relevant as they demonstrate novel molecular mechanism of two understudied molecules for potential therapeutic development. Targeting *CRYBB2* and *CRYBB2P1* may assist in reducing the disparate survival outcomes observed between Black and White American breast cancer patients, or may better identify those patients most at risk for more aggressive disease.

Additional files

Additional file 1: Table S1. Breast Cancer Cell lines and their associated race of origin and subtype. (PDF 82 kb)

Additional file 2: Table S2. qPCR Primer Sequences (PDF 37 kb)

Additional file 3: Figure S1. Distribution of each gene among subtype and race using linear regression: conditioning on race (a) or subtype (b). *CRYBB2* *adjusted $p = 0.00427$; *CRYBB2P1* *adjusted $p = 7.7E-05$, **adjusted $p = 1.3E-02$. e *CRYBB2P1* *adjusted $p = 0.0043$, **adjusted $p = 0.0008$. Distribution of *CRYBB2* and *CRYBB2P1* among race within subtype (c) and *CRYBB2P1* among age/menopausal status (d). Significant results for *CRYBB2* *adjusted $p = 0.0304$, and for *CRYBB2P1* *adjusted $p = 2.4E-06$, #adjusted $p = 5.3E-03$, and **adjusted $p = 2.3E-04$. d *CRYBB2P1* distribution among age before conditioning for race: *adjusted $p = 0.0334$, **adjusted $p = 0.0231$, #adjusted $p = 0.0052$, ##adjusted $p = 0.0269$, and (e) subtype after conditioning for race: * adjusted $p = 0.0071$, ** adjusted $p = 0.0369$, and #adjusted $p = 0.0257$. Young <40 yrs, Pre = pre-menopausal 40-46, Peri = peri-menopausal 46-55, and Post = post-menopausal >55 yrs. Figure S2. Distribution of transcript localization for each gene following subcellular fractionalization of RNAs. RNA was isolated and separated into cytosolic and nuclear subcellular fractions from proliferating cells. U6 and ACTB expression show successful separation of the nuclear and cytosolic subcellular compartments, respectively. 159 = SUM159, P-/- = *CRYBB2P1* knockout, C-/- = *CRYBB2* knockout, cyto = cytosolic fraction, nuc = nuclear fraction. Figure S3. *CRYBB2* alters breast cancer cell growth behaviors in 3D cell culture. a Cells were grown in Matrigel and imaged on day 8. Data is one representative assay of a minimum of four independent experiments from Hs578t models. Figure S4. Cells were grown to 80% confluence, washed, then incubated in serum-free media 24 h. Images are representative immunoblots from the indicated models of control parental or *CRYBB2*-overexpressing cells. All data represent a minimum of three independent experiments. +C = *CRYBB2* overexpression. Figure S5. *CRYBB2* and *CRYBB2P1* expression patterns of pancreatic cancer cell models. qRT-PCR analysis of the indicated cell lines. HPNE = hTERT-HPNE non-cancerous pancreatic ductal cells. Remaining cell models are pancreatic cancer cell lines. (PDF 5920 kb)

Abbreviations

ANOVA: Analysis of variance; CRISPR: Clustered regularly interspaced short palindromic repeats; *CRYBB2*: Crystallin beta B2; *CRYBB2P*: Crystallin beta B2 pseudogene 1; EMT: Epithelial-mesenchymal transition; HSD: Honestly significant difference; IL6: Interleukin 6; ncRNA: Non-coding RNA; NFkB: Nuclear factor kappa-light-chain-enhancer of activated B cells; SOX10: SRY-Box 10; STAT3: Signal transducer and activator of transcription 3; TCGA: The Cancer Genome Atlas

Authors' contributions

MAB, JSP, MAT, and JMF were involved in the design of the study. MAB, MEM, AC, DKR, PLA, JSP, MAT, and JMF were involved with the acquisition and interpretation of the data. GSJ, AC, MAT, and JSP conducted the statistical analyses. MAB, AC, JLP, MAT, and JMF conducted the analyses of the data and drafted the manuscript. All authors read and approved the final manuscript.

Funding

This work was supported [in part] by a grant from the University of North Carolina Lineberger Comprehensive Cancer Center, the NCI under Grant U54 CA156735, the Komen Foundation under Grant GTDR16377604, and the NIMHD under Grant U54 MD012392.

Availability of data and materials

Data used in this study are included in this published article and its supplementary files.

Ethics approval and consent to participate

Not applicable.

Consent for publication

Not applicable.

Competing interests

The authors declare that they have not competing interests.

Author details

¹Department of Biological and Biomedical Sciences, North Carolina Central University, 1801 Fayetteville Street, Mary Townes Science Complex, Durham, NC 27707, USA. ²Lineberger Comprehensive Cancer Center, University of North Carolina at Chapel Hill, Chapel Hill, NC, USA. ³Department of Genetics, University of North Carolina at Chapel Hill, Chapel Hill, NC, USA. ⁴Department of Epidemiology, University of North Carolina at Chapel Hill, Chapel Hill, NC, USA.

Received: 23 April 2019 Accepted: 28 August 2019

Published online: 11 September 2019

References

- DeSantis CE, Siegel RL, Sauer AG, Miller KD, Fedewa SA, Alcaraz KI, et al. Cancer statistics for African Americans, 2016: progress and opportunities in reducing racial disparities. *CA Cancer J Clin*. 2016;66(4):290–308.
- DeSantis CE, Ma J, Goding Sauer A, Newman LA, Jemal A. Breast cancer statistics, 2017, racial disparity in mortality by state. *CA Cancer J Clin*. 2017; 67(6):439–48.
- Warner ET, Tamimi RM, Hughes ME, Ottesen RA, Wong YN, Edge SB, et al. Racial and ethnic differences in breast cancer survival: mediating effect of tumor characteristics and sociodemographic and treatment factors. *J Clin Oncol*. 2015;33(20):2254–61.
- Wheeler SB, Reeder-Hayes KE, Carey LA. Disparities in breast cancer treatment and outcomes: biological, social, and health system determinants and opportunities for research. *Oncologist*. 2013;18(9):986–93.
- O'Brien KM, Cole SR, Tse CK, Perou CM, Carey LA, Foulkes WD, et al. Intrinsic breast tumor subtypes, race, and long-term survival in the Carolina Breast Cancer Study. *Clin Cancer Res*. 2010;16(24):6100–10.
- Carey LA, Perou CM, Livasy CA, Dressler LG, Cowan D, Conway K, et al. Race, breast cancer subtypes, and survival in the Carolina Breast Cancer Study. *JAMA*. 2006;295(21):2492–502.
- D'Arcy M, Fleming J, Robinson WR, Kirk EL, Perou CM, Troester MA. Race-associated biological differences among Luminal A breast tumors. *Breast Cancer Res Treat*. 2015;152(2):437–48.
- Huo D, Hu H, Rhie SK, Gamazon ER, Cherniack AD, Liu J, et al. Comparison of breast cancer molecular features and survival by African and European ancestry in The Cancer Genome Atlas. *JAMA Oncol*. 2017;3(12):1654–62.
- Troester MA, Sun X, Allott EH, Geradts J, Cohen SM, Tse CK, et al. Racial differences in PAM50 subtypes in the Carolina Breast Cancer Study. *J Natl Cancer Inst*. 2018;110(2):176–82.
- Daly B, Olopade OI. A perfect storm: how tumor biology, genomics, and health care delivery patterns collide to create a racial survival disparity in breast cancer and proposed interventions for change. *CA Cancer J Clin*. 2015;65(3):221–38.
- Parada H Jr, Sun X, Fleming JM, Williams-DeVane CR, Kirk EL, Olsson LT, et al. Race-associated biological differences among luminal A and basal-like breast cancers in the Carolina Breast Cancer Study. *Breast Cancer Res*. 2017;19(1):131.
- Wallace TA, Prueitt RL, Yi M, Howe TM, Gillespie JW, Yfantis HG, et al. Tumor immunobiological differences in prostate cancer between African-American and European-American men. *Cancer Res*. 2008;68(3):927–36.
- Grunda JM, Steg AD, He Q, Steciuk MR, Byan-Parker S, Johnson MR, et al. Differential expression of breast cancer-associated genes between stage- and age-matched tumor specimens from African- and Caucasian-American women diagnosed with breast cancer. *BMC Res Notes*. 2012;5:248.
- Field LA, Love B, Deyarmin B, Hooke JA, Shriver CD, Ellsworth RE. Identification of differentially expressed genes in breast tumors from African American compared with Caucasian women. *Cancer*. 2012;118(5):1334–44.
- Martin DN, Boersma BJ, Yi M, Reimers M, Howe TM, Yfantis HG, et al. Differences in the tumor microenvironment between African-American and European-American breast cancer patients. *PLoS One*. 2009;4(2):e4531.
- Paulucci DJ, Sfakianos JP, Skanderup AJ, Kan K, Tsao CK, Galsky MD, et al. Genomic differences between black and white patients implicate a distinct immune response to papillary renal cell carcinoma. *Oncotarget*. 2017;8(3): 5196–205.
- Wu M, Miska J, Xiao T, Zhang P, Kane JR, Balyasnikova IV, et al. Race influences survival in glioblastoma patients with KPS \geq 80 and associates

- with genetic markers of retinoic acid metabolism. *J Neurooncol*. 2019; 142(2):375–84.
18. Jovov B, Araujo-Perez F, Sigel CS, Stratford JK, McCoy AN, Yeh JJ, et al. Differential gene expression between African American and European American colorectal cancer patients. *PLoS One*. 2012;7(1):e30168.
 19. Astiazaran MC, Garcia-Montano LA, Sanchez-Moreno F, Matiz-Moreno H, Zenteno JC. Next generation sequencing-based molecular diagnosis in familial congenital cataract expands the mutational spectrum in known congenital cataract genes. *Am J Med Genet A*. 2018;176(12):2637–45.
 20. Sturgill GM, Bala E, Yaniglos SS, Peachey NS, Hagstrom SA. Mutation screen of beta-crystallin genes in 274 patients with age-related macular degeneration. *Ophthalmic Genet*. 2010;31(3):129–34.
 21. Gao Q, Sun LL, Xiang FF, Gao L, Jia Y, Zhang JR, et al. Crybb2 deficiency impairs fertility in female mice. *Biochem Biophys Res Commun*. 2014;453(1):37–42.
 22. Xiang F, Cui B, Gao Q, Zhang J, Zhang J, Li W. Decreased levels of Ca(2+)-calmodulin-dependent protein kinase IV in the testis as a contributing factor to reduced fertility in male Crybb2(-/-) mice. *Int J Mol Med*. 2012; 30(5):1145–51.
 23. Sturtz LA, Melley J, Mamula K, Shriver CD, Ellsworth RE. Outcome disparities in African American women with triple negative breast cancer: a comparison of epidemiological and molecular factors between African American and Caucasian women with triple negative breast cancer. *BMC Cancer*. 2014;14:62.
 24. Costantino NS, Freeman B, Shriver CD, Ellsworth RE. Outcome disparities in African American compared with European American women with ER+ HER2- tumors treated within an equal-access health care system. *Ethn Dis*. 2016;26(3):407–16.
 25. Hansen L, Rosenberg T. Author response: nonspecific PCR amplification of CRYBB2-pseudogene leads to misconception of natural variation as mutation. *Invest Ophthalmol Vis Sci*. 2012;53(10):6666.
 26. Kumar KD, Kumar GS, Santhiya ST. Nonspecific PCR amplification of CRYBB2-pseudogene leads to misconception of natural variation as mutation. *Invest Ophthalmol Vis Sci*. 2012;53(9):5770.
 27. Hansen L, Mikkelsen A, Nurnberg P, Nurnberg G, Anjum I, Eiberg H, et al. Comprehensive mutational screening in a cohort of Danish families with hereditary congenital cataract. *Invest Ophthalmol Vis Sci*. 2009;50(7):3291–303.
 28. Milligan MJ, Lipovich L. Pseudogene-derived lncRNAs: emerging regulators of gene expression. *Front Genet*. 2014;5:476.
 29. Reaves DK, Fagan-Solis KD, Dunphy K, Oliver SD, Scott DW, Fleming JM. The role of lipolysis stimulated lipoprotein receptor in breast cancer and directing breast cancer cell behavior. *PLoS One*. 2014;9(3):e91747.
 30. Fagan-Solis KD, Reaves DK, Rangel MC, Popoff MR, Stiles BG, Fleming JM. Challenging the roles of CD44 and lipolysis stimulated lipoprotein receptor in conveying Clostridium perfringens iota toxin cytotoxicity in breast cancer. *Mol Cancer*. 2014;13:163.
 31. Fleming JM, Miller TC, Kidacki M, Ginsburg E, Stuelten CH, Stewart DA, et al. Paracrine interactions between primary human macrophages and human fibroblasts enhance murine mammary gland humanization in vivo. *Breast Cancer Res*. 2012;14(3):R97.
 32. Reaves DK, Hoadley KA, Fagan-Solis K, Jima DD, Bereman M, Thorpe L, et al. Nuclear localized LSR, a novel regulator of breast cancer behavior and tumorigenesis. *Mo Cancer Res*. 2016;15(2):165–78.
 33. Fleming JM, Miller TC, Quinones M, Xiao Z, Xu X, Meyer MJ, et al. The normal breast microenvironment of premenopausal women differentially influences the behavior of breast cancer cells in vitro and in vivo. *BMC Med*. 2010;8:27.
 34. Debnath J, Muthuswamy SK, Brugge JS. Morphogenesis and oncogenesis of MCF-10A mammary epithelial acini grown in three-dimensional basement membrane cultures. *Methods*. 2003;30(3):256–68.
 35. Lee GY, Kenny PA, Lee EH, Bissell MJ. Three-dimensional culture models of normal and malignant breast epithelial cells. *Nat Methods*. 2007;4(4):359–65.
 36. Casbas-Hernandez P, D'Arcy M, Roman-Perez E, Brauer HA, McNaughton K, Miller SM, et al. Role of HGF in epithelial-stromal cell interactions during progression from benign breast disease to ductal carcinoma in situ. *Breast Cancer Res*. 2013;15(5):R82.
 37. Nieman KM, Kenny HA, Penicka CV, Ladanyi A, Buell-Gutbrod R, Zillhardt MR, et al. Adipocytes promote ovarian cancer metastasis and provide energy for rapid tumor growth. *Nat Med*. 2011;17(11):1498–503.
 38. Lock R, Kenific CM, Leidal AM, Salas E, Debnath J. Autophagy-dependent production of secreted factors facilitates oncogenic RAS-driven invasion. *Cancer Discov*. 2014;4(4):466–79.
 39. Deshmukh SK, Srivastava SK, Bhardwaj A, Singh AP, Tyagi N, Marimuthu S, et al. Resistin and interleukin-6 exhibit racially-disparate expression in breast cancer patients, display molecular association and promote growth and aggressiveness of tumor cells through STAT3 activation. *Oncotarget*. 2015; 6(13):11231–41.
 40. Park NJ, Kang DH. Inflammatory cytokine levels and breast cancer risk factors: racial differences of healthy Caucasian and African American women. *Oncol Nurs Forum*. 2013;40(5):490–500.
 41. Dethlefsen C, Hojfeldt G, Hojman P. The role of intratumoral and systemic IL-6 in breast cancer. *Breast Cancer Res Treat*. 2013;138(3):657–64.
 42. Korneev SA, Park JH, O'Shea M. Neuronal expression of neural nitric oxide synthase (nNOS) protein is suppressed by an antisense RNA transcribed from an NOS pseudogene. *J Neurosci*. 1999;19(18):7711–20.
 43. Duret L, Chureau C, Samain S, Weissenbach J, Avner P. The Xist RNA gene evolved in eutherians by pseudogenization of a protein-coding gene. *Science*. 2006;312(5780):1653–5.
 44. Li W, Yang W, Wang XJ. Pseudogenes: pseudo or real functional elements? *J Genet Genomics*. 2013;40(4):171–7.
 45. Rapicavoli NA, Qu K, Zhang J, Mikhail M, Laberge RM, Chang HY. A mammalian pseudogene lncRNA at the interface of inflammation and anti-inflammatory therapeutics. *eLife*. 2013;2:e00762.
 46. Chavez KJ, Garimella SV, Lipkowitz S. Triple negative breast cancer cell lines: one tool in the search for better treatment of triple negative breast cancer. *Breast Dis*. 2010;32(1–2):35–48.
 47. Prat A, Adamo B, Cheang MC, Anders CK, Carey LA, Perou CM. Molecular characterization of basal-like and non-basal-like triple-negative breast cancer. *Oncologist*. 2013;18(2):123–33.
 48. Prat A, Adamo B, Fan C, Peg V, Vidal M, Galvan P, et al. Genomic analyses across six cancer types identify basal-like breast cancer as a unique molecular entity. *Sci Rep*. 2013;3:3544.
 49. Lehmann BD, Bauer JA, Chen X, Sanders ME, Chakravarthy AB, Shyr Y, et al. Identification of human triple-negative breast cancer subtypes and preclinical models for selection of targeted therapies. *J Clin Invest*. 2011; 121(7):2750–67.
 50. Dravis C, Chung CY, Lytle NK, Herrera-Valdez J, Luna G, Trejo CL, et al. Epigenetic and transcriptomic profiling of mammary gland development and tumor models disclose regulators of cell state plasticity. *Cancer Cell*. 2018;34(3):466–82 e6.

Publisher's Note

Springer Nature remains neutral with regard to jurisdictional claims in published maps and institutional affiliations.

Ready to submit your research? Choose BMC and benefit from:

- fast, convenient online submission
- thorough peer review by experienced researchers in your field
- rapid publication on acceptance
- support for research data, including large and complex data types
- gold Open Access which fosters wider collaboration and increased citations
- maximum visibility for your research: over 100M website views per year

At BMC, research is always in progress.

Learn more biomedcentral.com/submissions

